

## NMR Spectroscopy of Experimentally Shocked Quartz: Shock Wave Barometry

R. T. Cygan

Geochemistry Division, Sandia National Laboratories,  
Albuquerque, NM 87185

M. B. Boslough

Shock Wave and Structural Physics Division, Sandia National Laboratories,  
Albuquerque, NM 87185

R. J. Kirkpatrick

Department of Geology, University of Illinois,  
Urbana, IL 61801

---

<sup>29</sup>Si MAS NMR spectra of synthetic quartz powders recovered from shock experiments at mean pressures of 7.5, 16.5, and 22 GPa indicate that the NMR technique is very sensitive to shock pressure. All of the shocked powders and the starting material have similar values for the refractive indices. The (101) X-ray diffraction peak of quartz broadens only slightly with shock pressure, at most by a factor of 1.7. By comparison, the <sup>29</sup>Si NMR spectra exhibit a nearly fivefold increase in relative peak width at the highest shock pressure. The broadening of the NMR peak is most likely the result of disordering and residual strain in the quartz lattice and the formation of an amorphous silica phase. The calibration of the NMR peak widths with shock pressure provides a very sensitive shock barometer for the determination of pressures associated with natural impacts, as well as materials subjected to shock by nuclear tests.

### INTRODUCTION

The shock-loading of natural materials by impact can result in the formation of highly modified phases. Shocked minerals typically exhibit fracturing, planar deformation, comminution, disordering, lamellae, and, frequently, new phases. These new phases may be glass (fused or diaplectic) or other reaction products that include high-pressure polymorphs of the original minerals (see *Stöffler*, 1984). For a given material the extent to which these shock-induced features form depends upon the peak shock pressures and temperatures. These variables, in turn, are related to velocity, composition, density, and angle of impact associated with the projectile, and the original composition and density (porosity) of the target material. The modifications and changes in the original material induced by the shock are referred to as shock metamorphism.

The effects of shock metamorphism on minerals, in particular the presence of the high-pressure polymorphs of SiO<sub>2</sub> (coesite and stishovite), have been used to identify impact events (*Stöffler*, 1971). For the Meteor Crater, Arizona, terrestrial impact site, the occurrence and textural relationships of glass and the SiO<sub>2</sub> polymorphs have provided a basis for estimating the shock pressure (*Kieffer*, 1971; *Kieffer et al.*, 1976).

Recent interest in an extraterrestrial cause for the Cretaceous-Tertiary extinction (*Alvarez et al.*, 1980) has prompted an increase in research on shock features in quartz (for example, *Bobor et al.*, 1984; *Carter et al.*, 1986; *Alexopoulos et al.*, 1988). The *Alvarez et al.* (1980) theory proposed that a large asteroid collided with the Earth 65 m.y. ago, resulting in mass extinctions. Observed shock features in mineral grains and possible stishovite in clay layers from near

the Cretaceous-Tertiary boundary support this idea (*Bobor et al.*, 1984; *McHone et al.*, 1989). However, several researchers interpret shock features in minerals to be the result of volcanic eruption processes (*Carter et al.*, 1986), but this interpretation remains controversial and is not generally accepted (*Izett and Bobor*, 1987; *Sbarpton and Schuraytz*, 1989). Multiple sets of shock lamellae and reduced values of the refractive indices are widely accepted as diagnostic of a shock event in the minerals.

Studies of the effect of shock in minerals have traditionally relied on qualitative examination of microstructures by optical and electron microscopies. Refractivity, density, X-ray diffraction, infrared absorption, X-ray photoelectron spectroscopy, and electron paramagnetic resonance (EPR) have been used to quantify the physical state of shocked minerals and glasses (see *Stöffler*, 1984). Optical refractivity has proven to be one of the most useful diagnostic techniques of shock metamorphism, especially for quartz (*Cbao*, 1968; *Hörz*, 1968). Its usefulness as a shock barometer was determined by recent spindle stage measurements, which show a decrease in birefringence and refractive index for material shocked to pressures above 22 GPa (*Grothues et al.*, 1989). Above shock pressures of 28 GPa, quartz becomes increasingly isotropic and completely transforms to diaplectic glass at 35 GPa, but at pressures below 22 GPa there is little change in the refractive indices (Fig. 1). Detailed X-ray line broadening studies of shocked powder and single crystal quartz have also been performed and indicate a decrease in domain size and an increase in microstrain effects with increasing shock pressure (*Hörz and Quaide*, 1973; *Schneider et al.*, 1984; *Asbworth and Schneider*, 1985). Because these microstructural properties are apparently a function of shock pressure, X-ray line broadening may also be used as a shock barometer.

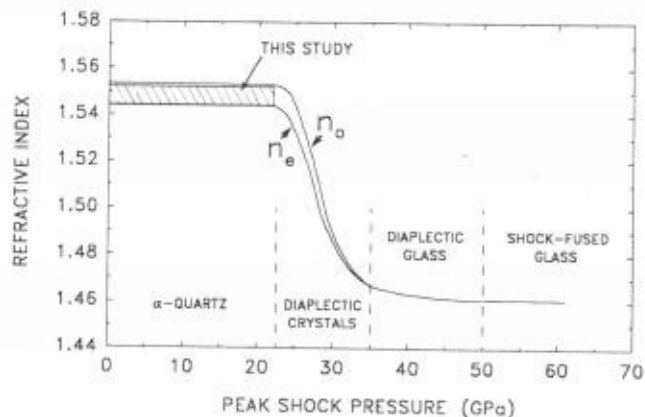


Fig. 1. Refractive index as a function of peak shock pressure, demonstrating the decrease in refractivity and birefringence with increasing shock pressure. The curves labeled  $n_o$  and  $n_e$  define the birefringence envelope for shocked single crystals of quartz (Grothues *et al.*, 1989). The ordinary index,  $n_o$ , and extraordinary index,  $n_e$ , begin to converge at shock pressures greater than 22 GPa and eventually coalesce at a shock pressure of about 35 GPa to indicate the formation of an isotropic phase (diaplectic glass). The refractivity measurements from the present study are for shocked powder samples.

In an attempt to better understand the structural changes in quartz with shock-loading and to develop a better measure of shock pressure, we use solid state  $^{29}\text{Si}$  nuclear magnetic resonance (NMR) spectroscopy to examine quartz powders shocked to pressures of 7.5-22 GPa. This NMR technique involves monitoring radio frequency reemissions from  $^{29}\text{Si}$  nuclei while the sample is in a very strong magnetic field (see Kirkpatrick, 1988). The resonance frequencies are sensitive to the local electronic (that is, structural) environment of silicon in the material, and thus provide information about the range of silicon environments resulting from, for instance, shock modification. One aim of this research is to provide a sensitive technique for monitoring shock pressure by calibrating a  $^{29}\text{Si}$  NMR shock wave barometer.

NMR spectroscopy is useful in the analysis of shocked quartz because of the sensitivity of the NMR frequencies to the local (nearest and next-nearest neighbor) environment of the  $^{29}\text{Si}$ . The resonance frequencies are reported as chemical shifts, which are ppm deviations of the resonance frequency from that of a standard (tetramethylsilane in this case). The  $^{29}\text{Si}$  resonances of  $\text{SiO}_2$  have been examined by Smith and Blackwell (1983), Oestrike *et al.* (1987), and Murdoch *et al.* (1985) among many others. These studies have determined the chemical shifts for the silicon sites in quartz, fused glass, coesite, and stishovite. Yang *et al.* (1986) examined shocked Coconino sandstone from Meteor Crater, Arizona, and identified the characteristic  $^{29}\text{Si}$  resonances of quartz, coesite, and stishovite. Figure 2 provides several NMR spectra of these materials for reference. Stishovite has a very different chemical shift because its silicon is in sixfold coordination, and the electronic shielding is much different. The coesite structure has two tetrahedral silicon sites, one of which has a chemical shift close to that of quartz.

Recently, McHone *et al.* (1989) used  $^{29}\text{Si}$  MAS NMR to identify stishovite in a concentrated sample of a Cretaceous-Tertiary boundary clay from Raton, New Mexico. This result provides support for the hypothesis that the impact of an extraterrestrial object led to the Cretaceous-Tertiary extinction. McHone and Nieman (1988) also identified stishovite by  $^{29}\text{Si}$  NMR in material from the Vredefort Dome of South Africa, which has been proposed to be an impact feature.

Application of the NMR technique to the shocked quartz powders is thus attractive due to the potential of NMR to distinguish among the amorphous, cryptocrystalline, and crystalline phases that may exist in bulk samples. Early studies of the shock-loading of quartz (De Carli and Jamieson, 1959; De Carli and Milton, 1965; Deribas *et al.*, 1965) recognized the presence of stable and metastable silica phases including fused and diaplectic glasses and the high-pressure polymorphs. NMR analysis provides a unique capability for identifying these phases based upon the local structural environment of silicon.

## EXPERIMENTAL METHODS

The shock recovery experiments on quartz powder were performed using the Sandia "Bear" explosive loading fixtures to provide well-characterized shock states. The recovery fixtures allow samples to be shocked in a controlled and reproducible manner. Peak shock pressures and temperatures are determined by numerical simulations. Grabam and Webb (1984, 1986) provide details of the experimental shock-loading experiment and the numerical simulations. Mean-bulk shock temperatures are determined in part by the initial packing density of the mineral powders. The mean peak shock pressures are 7.5, 16.5, and 22 GPa, and the mean bulk

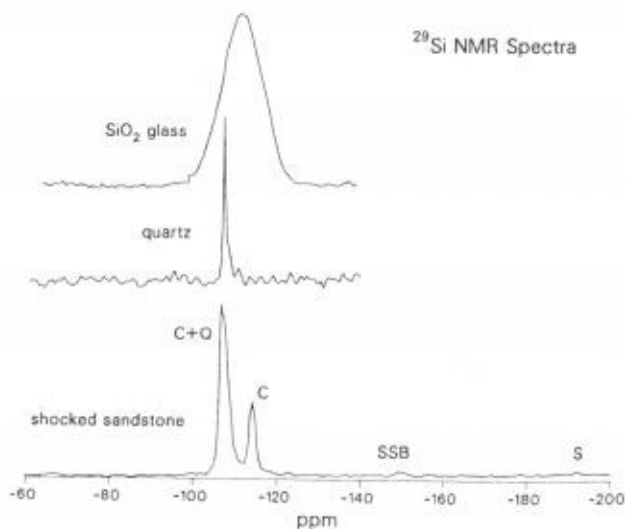


Fig. 2.  $^{29}\text{Si}$  MAS NMR spectra of  $\text{SiO}_2$  glass, quartz, and a naturally shocked sandstone from Meteor Crater, Arizona (modified from Yang *et al.*, 1986 and Oestrike *et al.*, 1987). The resonance frequencies are presented in ppm relative to the standard resonance of  $^{29}\text{Si}$  in tetramethylsilane. Coesite (C), quartz (Q), and stishovite (S) are noted in the shocked sandstone spectrum. Spinning sidebands (SSB) are the result of the MAS technique.

TABLE 1. Schedule of shock recovery experiments.

Shot	Fixture	Explosive	Sample Compact Density (Mg/m <sup>3</sup> )	Sample Compact Density (%)	Peak Pressure (GPa)	Estimated Mean Bulk Temperature (°C)
7B866	Momma Bear	Baratol	1.6	60	5-10	150-175
8B866	Momma Bear-A	Comp B	1.6	60	18-26	325-575
9B866	Momma Bear	Comp B	1.6	60	13-20	325-475
10B866	Momma Bear	Baratol	1.3	50	5-10	325-350
11B866	Momma Bear-A	Comp B	1.3	50	18-26	475-700
12B866	Momma Bear	Comp B	1.3	50	13-20	475-600

temperatures range from 150°C to 700°C. The range of pressures and temperatures presented in Table 1 are due to nonuniaxial loading; the variables have a radial dependence as determined by the numerical simulations. Samples to be analyzed were taken from a region with weak radial dependence (according to the simulations) and with pressures and temperatures close to the mean values. The use of two different packing densities for each shock pressure provided a low and a high temperature set of shocked samples.

The starting material for the shock-loading experiments was synthetic  $\alpha$ -quartz powder (<325 mesh) obtained from Alfa Products (lot #88316). The material was briefly washed with deionized water and dried before insertion in the shock recovery sample holder; approximately 8 g of the quartz powder was required for each experiment. X-ray diffraction analysis of the starting material indicated pure, single phase  $\alpha$ -quartz with no amorphous or glassy material present. Scanning electron microscopic (SEM) examination of the starting material determined a size distribution of approximately 30 to 90  $\mu\text{m}$ . After removal from the recovery fixtures, the shocked material was lightly disaggregated with a mortar and pestle. Approximately 200-300 mg of powder sample are required for NMR analysis, and an additional 1-g sample was used for optical, SEM, and X-ray diffraction examinations.

Refractive index measurements were performed using a standard optical microscope with sodium light, standard immersion oils at 23°C, and the method of central illumination. The refractivity values are presented as a range of values because of variable orientation of the anisotropic grains. The restricted values of immersion oil standards limit the accuracy of the refractivity measurements to 0.004.

The X-ray diffraction patterns were obtained using Cu K $\alpha$  X-ray radiation and a Phillips diffractometer with powders prepared on aluminum slides. Diffraction scans were performed from 10° to 70° 2 $\theta$  at a scan rate of 2° 2 $\theta$ /min and from 26° to 27° 2 $\theta$  at a scan rate of 0.25° 2 $\theta$ /min. The latter scan provides more detail of the shape of the quartz (101) peak.

The <sup>29</sup>Si NMR spectra were obtained at a frequency of 71.5 MHz ( $H_0 = 8.45$  T) under magic-angle spinning (MAS) conditions (see Yang et al., 1986; Kirkpatrick et al., 1986; Oestrike et al., 1987; Kirkpatrick, 1988). MAS frequencies were typically 2.8 kHz. A pulse Fourier transform method was used to obtain the NMR spectra by first detecting signals in the time domain, then transforming the data to yield spectra in the frequency domain.

## RESULTS

SEM examination of our shocked quartz powders indicates that substantial brittle disaggregation occurred due to shock-loading. Significant comminution, deformation, and fracturing is apparent. The mean grain size was reduced from 30-90  $\mu\text{m}$  to 10-60  $\mu\text{m}$  in all cases. Fine-grained (less than 1  $\mu\text{m}$ ) material is more abundant in the shocked quartz samples than in the unshocked sample. Small blebs (5-15  $\mu\text{m}$ ) of apparently amorphous material occur in the 22 GPa samples. Planar features (shock lamellae) were observed in only the low-temperature 22-GPa sample. One quartz grain in the sample contains three sets of parallel structural voids visible after hydrofluoric acid treatment. Presumably, the HF preferentially etches the diaplectic glass that fills the shock lamellae (Bobor et al., 1984).

Within the precision of the measurement technique, there is no variation in the refractive indices of the shocked samples, and the measured refractive indices were all identical to the unshocked quartz sample (Fig. 1). Mean peak shock pressures for these samples are below that required to affect the refractive index.

The full X-ray diffraction scans for each of the shocked powders indicate the presence of only quartz. There is no evidence of a broad glass peak near 25° 2 $\theta$ . The detailed scans of the most intense quartz peak (101) at 26.6° 2 $\theta$  show a small but measurable broadening with increasing shock pressure for both the low- and high-temperature runs (Fig. 3). There is also a shift in peak position toward lower 2 $\theta$  values (larger d-spacing) with increased shock pressure up to 16 GPa. There is no shift in the peak position for either of the 22 GPa samples.

The NMR spectra are characterized by a single peak with a maximum of about -108 ppm for four-coordinated <sup>29</sup>Si in quartz. However, this peak broadens substantially with increasing shock pressure (Fig. 4). The unshocked quartz has a full-width-at-half-height (FWHH) of 0.8 ppm, whereas that of the high-temperature 22-GPa sample is 3.8 ppm. The peaks of the high-temperature samples are somewhat more broadened than those of the low-temperature samples. There is no peak for stishovite, which would occur at about -192 ppm (Smith and Blackwell, 1983; Yang et al., 1986), consistent with the relatively low pressures of our shock experiments. In addition, the NMR peak maxima tend to shift upfield (to lower frequencies or less negative chemical shifts) with increasing shock pressure. The only exception to this trend is the lower



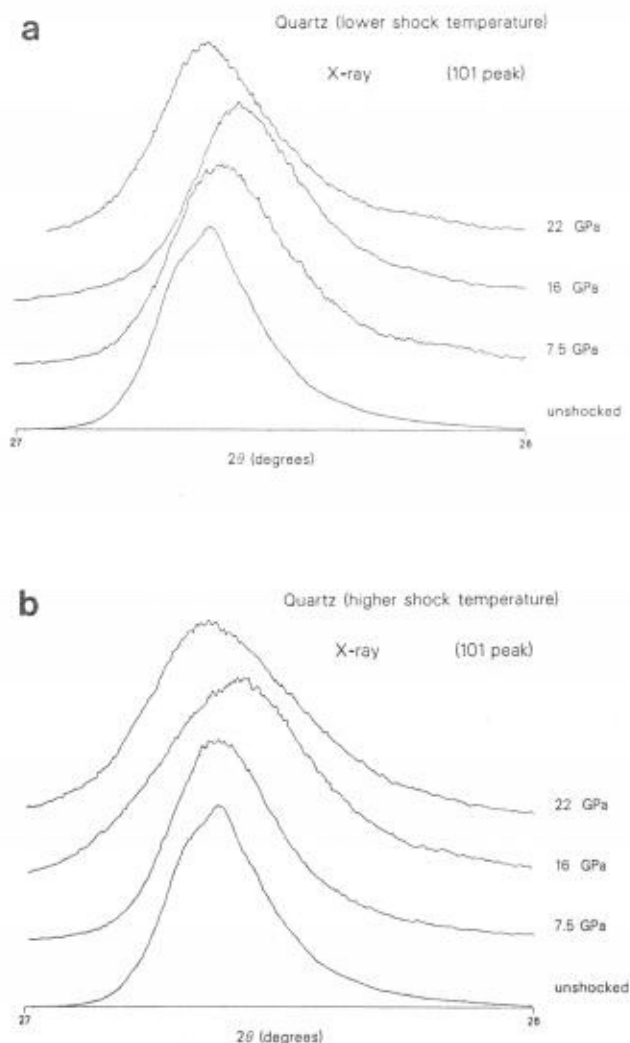


**Fig. 3.** Comparison of the X-ray diffraction patterns for the  $26.6^\circ$   $2\theta$  peak (101) for the shocked quartz powders relative to that for the unshocked starting material: (a) low shock temperature samples and (b) high shock temperature samples. Diffraction patterns were obtained at a scan rate of  $0.25^\circ$   $2\theta/\text{min}$ .

temperature 22-GPa sample, which is shifted upfield relative to the unshocked sample but not as far as the 16-GPa sample. This behavior is similar to the shifts in  $2\theta$  observed in the X-ray diffraction patterns for the same 22-GPa shocked samples.

## DISCUSSION

### X-ray Diffraction

Broadening of X-ray diffraction lines usually is associated with residual strain, disorder of the crystal, and decrease of crystal domain size (Hörz and Quaide, 1973; Schneider et al., 1984). Shifts in diffraction peaks by lattice strain effects usually represent uniform strain whereas broadening of the peaks indicates a nonuniform strain (Cullity, 1978). We are uncertain how to interpret the X-ray diffraction data of the 22-GPa samples (see Fig. 3). It is possible that these samples

experienced high enough temperatures (greater than  $570^\circ\text{C}$ ) during (and after) shock-loading that an inversion to  $\beta$ -quartz occurred that later reverted to the  $\alpha$ -quartz structure upon cooling.

The unshocked starting material possesses a fairly broad (101) X-ray peak indicating some inherent strain prior to shock-loading (F. Hörz, personal communication, 1989). This strain may have been generated during the initial synthesis and grinding of the material. However, all of the X-ray and NMR results are normalized relative to the starting material. A comparison of the sensitivity of the two techniques in quantifying the degree of disorder can therefore be made regardless of the initial state of the material. We hope to study this preshock effect in future research by examining a variety of synthetic, natural, and thermally annealed quartz samples.

### Nuclear Magnetic Resonance

The broadening of the NMR peak of the shocked quartz may be due to several different causes, but must be due to an increase in the range of mean Si-O-Si bond angle per silicon tetrahedron in the samples. Many workers, including Smith and Blackwell (1983), Dupree and Pettifer (1984), and Oestrike et al. (1987), have described the excellent relationship between this and the  $^{29}\text{Si}$  chemical shift for  $\text{SiO}_2$  phases.

One possible cause for this broadening is extensive disorder and residual strain introduced into the quartz lattice by shock-loading. Dupree and Pettifer (1984) and Devine et al. (1987) have suggested that such NMR peak broadening ultimately results from the redistribution of Si-O-Si bond angles that forms in response to stress. Although static pressures were used in the previous studies of amorphous silica phases, a similar argument can be made for the dynamic stressing of our study.

A second possible cause for the observed NMR peak broadening is formation of an amorphous phase. Vitreous silica has a  $^{29}\text{Si}$  resonance maximum at  $-111$  to  $-112$  ppm, and a FWHM of about 20 ppm (Dupree and Pettifer, 1984; Oestrike et al., 1987) (Fig. 2). The extent of such a contribution to the NMR spectra in Fig. 4 is uncertain. The asymmetrical shape of the peaks and the intensity in the  $-109$  to  $-118$  ppm range in the spectra of the high-pressure shock samples is consistent with some contribution from a silica glass phase. The intensity of this broad component increases with increasing shock pressure. Although none of the X-ray diffraction scans provide evidence of glass, our SEM observations confirm the existence of a glass phase in the shocked samples. NMR spectroscopy probably cannot discern between fused and diaplectic glasses of similar compositions or silicon coordinations.

A third possible cause of the peak broadening could be the presence of coesite, one of the high-pressure polymorphs of silica (Stöffler, 1971, 1984). Smith and Blackwell (1983) and Yang et al. (1986) observed two  $^{29}\text{Si}$  NMR peaks of  $-108.1$  ppm and  $-113.9$  ppm for this phase. Although no coesite is detected by X-ray diffraction, if coesite were formed it may have been in an amount below the detection level. It is possible that some coesite contributes to the peak broadening observed in Fig. 4.

An example of a possible deconvolution of the broadened NMR peak is presented in Fig. 5 where the relative contributions of the disordered quartz and silica glass may be graphically examined. An unidentified peak of low intensity

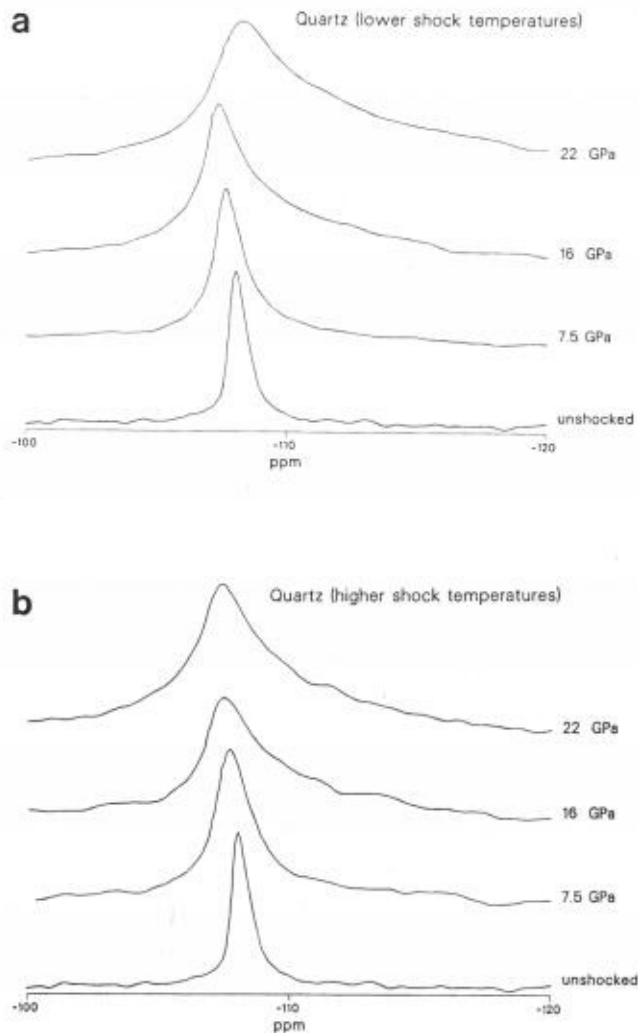


Fig. 4.  $^{29}\text{Si}$  MAS NMR spectra for shocked quartz powders relative to that for the unshocked starting material: (a) low shock temperature samples and (b) high shock temperature samples.

occurs upfield as a result of the optimum fitting of Gaussian curves to the NMR spectrum. In this model deconvolution, the optimum fit attributes about 60% of the  $^{29}\text{Si}$  NMR signal to the glass phase, whereas the disordered quartz accounts for 25% of the observed NMR peak. Because of the lack of singularities for constraining the model, the resulting curves do not necessarily represent a unique solution.

#### Relative Peak Changes and Shock Wave Barometry

Although the origin of the NMR peak broadening is not entirely clear, this broadening appears to be a useful empirical measure of peak shock pressures. Figure 6 shows that the NMR peak broadening increases much more rapidly with increasing shock pressure than X-ray diffraction peak broadening. The NMR peaks of the 22-GPa samples are almost five times broader than that of the unshocked quartz sample. The broadening of the NMR peaks shows no strong or consistent correlation with shock temperature.

The X-ray peak broadening increases at most by a factor of 1.7 relative to the unshocked samples and is much less than for the NMR peak widths (Fig. 6). This result suggests that NMR is a more sensitive measure of shock pressure. However, the synthetic quartz we used already had measurable line broadening in its unshocked state. For unstrained starting material, the X-ray line broadening may exhibit a stronger and more consistent trend than what we observed, but the NMR trend may also be enhanced.

The variation of the NMR peak widths with temperature is much smaller than that with pressure. Thus, the NMR peak width measurement can provide a shock barometer over a wide range of unknown shock temperatures. It may therefore be particularly useful in studies of naturally shocked quartz where the precise initial conditions and loading path (which dictate the shock temperature) are unknown.

One of the limitations in assessing the suitability of the NMR shock wave barometer is the uncertainty in the amount of glass and coesite generated during the experimental shock event. SEM examination of the shocked samples suggests that both fused and diaplectic glass are present. The NMR results indicate that these glasses contain only four-coordinated silicon and contribute to a broad peak with a mean chemical shift of approximately -110 ppm. Any higher coordinated silicon, such as a six-coordinated silicon in a stishovite-like diaplectic glass (Chaabildas and Miller, 1985; Boslough, 1988), would yield a resonance in the -190 to -200 ppm range and is not observed. Coesite or a disordered coesite-like material with mean Si-O-Si bond angles larger than quartz, and then more negative chemical shift, might also contribute to the observed peaks. Our NMR analysis of the low-temperature 22-GPa sample after treatment with hydrofluoric acid indicated an almost twofold decrease in FWHH relative to the untreated 22-GPa sample. The  $^{29}\text{Si}$  NMR spectrum exhibits some spectral intensity in the -114 ppm region where coesite would have a resonance (Smith and Blackwell, 1983; Yang et al., 1986). Future research will require improved NMR spectra with better signal-to-noise ratios and an analysis of standard mixtures of the quartz, coesite, and glass.

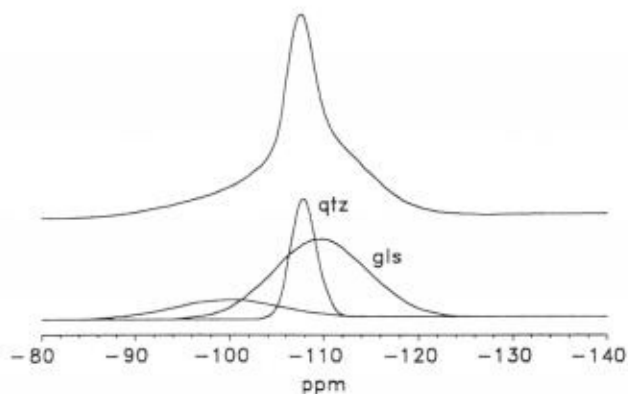


Fig. 5. Optimum curve fits for the  $^{29}\text{Si}$  MAS NMR spectrum for the high-temperature 22-GPa shocked quartz sample. The upper curve is a smoothed peak derived from the raw data. The lower curves provide the results of a possible deconvolution assuming 100% Gaussian peak shape for quartz, glass, and a third unidentified peak.

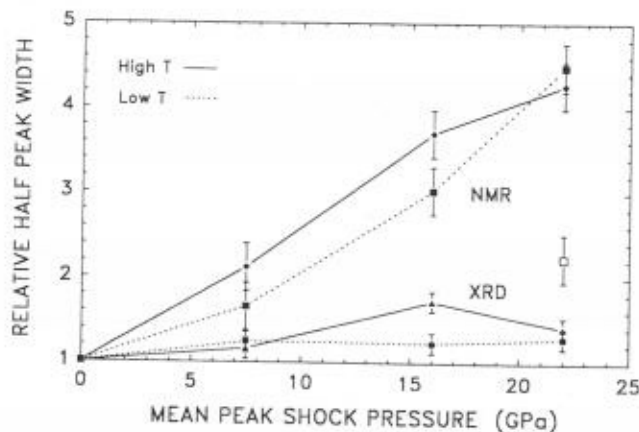


Fig. 6. Comparison of relative half-peak widths (full-width-at-half-height) obtained for X-ray diffraction (XRD) patterns and MAS NMR spectra of the shocked quartz powders as functions of the mean peak shock pressure. The open square indicates the NMR result for a low-temperature sample that was improperly selected.

#### Applications of the NMR Shock Wave Barometer

In applying an NMR shock barometer to terrestrial impact events, it is important to recognize the way the impact occurs and the amounts of material that are shocked by the impact. The amount of terrestrial material shocked to a given pressure by a meteoroid impact is a complex function of projectile mass, velocity, density, angle of impact, and other parameters. The highest shock pressures are in the small central region of the impact, and the material associated with the lower shock pressures is radially distant from the impact point, but represents a larger volume. The significant radial decay of shock pressure from the impact point therefore produces large volumes of material subjected to pressures less than 22 GPa (for example, *Stöffler, 1984*). An NMR shock barometer would be useful in determining the low shock pressures associated with this material. This is a significant advantage because refractive index-based shock barometers are limited to pressures greater than 22 GPa.

Another potential application of shock barometry using the NMR spectroscopic approach is the accurate scaling of stress decay associated with nuclear testing. The technique is amenable to postdetonation analysis of shock pressure exposure of rock samples. This method can be used in conjunction with real-time stress probes and sensors that collect data during the detonation, or for postdetonation analysis where real-time evaluation has failed or is lacking. Consequently, data from nuclear test sites can be used to calibrate natural shock events. This is similar to the approach of *Vizgirda et al. (1980)*, who examined the hyperfine EPR splitting of  $Mn^{2+}$  in calcite from shocked coral samples from Cactus crater at the Pacific test site. These results, however, do not conclusively define a reproducible trend between hyperfine peak splitting and shock pressure. We believe an NMR shock barometer would be more useful, because of the larger observed spectral changes and the widespread occurrence of quartz and other silicate minerals.

Future research on shocked material using MAS NMR spectroscopy should emphasize the structural differences associated with  $^{29}Si$  in diaplectic and fused glasses. Mineral samples should also be subjected to greater shock pressures in order to examine any coordination changes that may result. Although the present study has emphasized  $^{29}Si$  NMR spectroscopy, there are other NMR-active nuclei ( $^{23}Na$ ,  $^{27}Al$ , and  $^{39}K$ ) that could provide detailed information on the disordered state of other shocked minerals that may be present on the Moon and terrestrial planets. The maskelynitization of feldspar minerals could be examined in this fashion.

#### CONCLUSIONS

This study demonstrates a significant positive correlation of  $^{29}Si$  MAS NMR peak width with mean peak shock pressure for samples of synthetic quartz shocked up to 22 GPa and 700°C. The NMR technique is more sensitive to shock pressure than X-ray diffraction methods, with the (101) quartz X-ray peak broadening much less than the NMR peak for the synthetic quartz samples. The quartz refractive indices do not change in this low-pressure range, in agreement with the results of *Grothues et al. (1989)*. The results of this study suggest the potential usefulness of NMR spectroscopy in providing a shock barometer that is sensitive and accurate for shock pressures below 22 GPa. No other observable parameter appears to change as much or as consistently in this pressure range.

**Acknowledgments.** We wish to acknowledge the comments and careful reviews provided by F. Hörz and V. L. Sharpton. We also thank B. Montez for his exacting method in obtaining the MAS NMR spectra and C. Daniel, K. Elsner, and M. Anderson for their technical support with the shock recovery experiments. Additional technical support and scientific comments were provided by W. Casey, M. Dvorack, and B. Morosin. This research was performed at Sandia National Laboratories and was supported by the U.S. Department of Energy under contract DE-AC04-76DP00789.

#### REFERENCES

- Alexopoulos J. S., Grieve R. A. E., and Robertson P. B. (1988) Microscopic lamellar deformation features in quartz: Discriminative characteristics of shock-generated varieties. *Geology*, 16, 796-799.
- Alvarez L. W., Alvarez W., Asaro F., and Michel H. V. (1980) Extraterrestrial cause for the Cretaceous-Tertiary extinction. *Science*, 208, 1095-1108.
- Ashworth J. R. and Schneider H. (1985) Deformation and transformation in experimentally shock-loaded quartz. *Phys. Chem. Minerals*, 11, 241-249.
- Bohor B. E., Foord E. E., Modreski P. J., and Triplehorn D. M. (1984) Mineralogic evidence for an impact event at the Cretaceous-Tertiary boundary. *Science*, 224, 867-869.
- Boslough M. B. (1988) Postshock temperatures in silica. *J. Geophys. Res.*, 93, 6477-6484.
- Carter N. L., Officer C. B., Chesner C. A., and Rose W. I. (1986) Dynamic deformation of volcanic ejecta from the Toba caldera: Possible relevance to Cretaceous/Tertiary boundary phenomena. *Geology*, 14, 380-383.
- Chaabildas L. C. and Miller J. M. (1985) Release-adiabat measurements in crystalline quartz. *Sandia Rep. SAND85-1092*, Sandia National Laboratories, New Mexico. 26 pp.

- Chao E. C. T. (1968) Pressure and temperature histories of impact metamorphosed rocks—based on petrographic observations. In *Shock Metamorphism of Natural Materials* (B. M. French and N. M. Short, eds.), pp. 135-158. Mono, Baltimore.
- Cullity B. D. (1978) *Elements of X-Ray Diffraction*. Addison-Wesley, Reading, Massachusetts. 555 pp.
- De Carli P. S. and Jamieson J. C. (1959) Formation of an amorphous form of quartz under shock conditions. *J. Chem. Phys.*, 31, 1675-1676.
- De Carli P. S. and Milton D. J. (1965) Stishovite: Synthesis by shock wave. *Science*, 147, 144-145.
- Deribas A. A., Dobretsov N. L., Kudinov V. M., and Zyuzin N. I. (1965) Shock compression of SiO<sub>2</sub> powders. *Dok. Akad. Nauk SSSR*, 168, 127-130.
- Devine R. A. B., Dupree R., Farnan I., and Capponi J. J. (1987) Pressure-induced bond-angle variation in amorphous SiO<sub>2</sub>. *Phys. Rev. B*, 35, 2560-2562.
- Dupree E. and Pettifer R. F. (1984) Determination of Si-O-Si bond angle distribution in vitreous silica by magic angle spinning NMR. *Nature*, 308, 523-525.
- Graham R. A. and Webb D. M. (1984) Fixtures for controlled explosive loading and preservation of powder samples. In *Shock Waves in Condensed Matter—1983* (J. R. Asay, R. A. Graham, and G. K. Straub, eds.), pp. 211-214. North Holland, New York.
- Graham R. A. and Webb D. M. (1986) Shock-induced temperature distributions in powder compact recovery fixtures. In *Shock Waves in Condensed Matter—1985* (Y. M. Gupta, ed.), pp. 831-836. Plenum, New York.
- Grothues J., Hornemann U., and Stöffler D. (1989) Mineralogical shock wave barometry: (I) Calibration of refractive index data of experimentally shocked  $\alpha$ -quartz (abstract). In *Lunar and Planetary Science XX*, pp. 365-366. Lunar and Planetary Institute, Houston.
- Hörz F. (1968) Statistical measurements of deformation structures and refractive indices in experimentally shock loaded quartz. In *Shock Metamorphism of Natural Materials* (B. M. French and N. M. Short, eds.), pp. 243-253. Mono, Baltimore.
- Hörz F. and Quaide W. L. (1973) Debye-Scherrer investigations of experimentally shocked silicates. *The Moon*, 6, 45-82.
- Izett G. A. and Bohor B. F. (1987) Comment and reply on "Dynamic deformation of volcanic ejecta from the Toba caldera: Possible relevance to Cretaceous/Tertiary boundary phenomena." *Geology*, 15, 90-91.
- Kieffer S. W. (1971) Shock metamorphism of the Coconino Sandstone at Meteor Crater, Arizona. *J. Geophys. Res.*, 76, 5449-5473.
- Kieffer S. W., Phakey P. P., and Christie J. M. (1976) Shock processes in porous quartzite: Transmission electron microscope observations and theory. *Contrib. Mineral. Petrol.*, 59, 41-93.
- Kirkpatrick R. J. (1988) MAS NMR spectroscopy of minerals and glasses. In *Spectroscopic Methods in Mineralogy and Geology, Reviews in Mineralogy, Vol. 18* (E. C. Hawthorne, ed.), pp. 341-403. Mineralogical Society of America, Washington, DC.
- Kirkpatrick R. J., Dunn T., Schramm S., Smith K. A., Oestrike R., and Turner G. (1986) Magic-angle sample-spinning nuclear magnetic resonance spectroscopy of silicate glasses: A review. In *Structure and Bonding in Noncrystalline Solids* (G. E. Walrafen and A. G. Revesz, eds.), pp. 303-327. Plenum, New York.
- McHone J. E. and Nieman R. A. (1988) Vredefort stishovite confirmed using solid-state silicon-29 nuclear magnetic resonance. *Meteoritics*, 23, 289.
- McHone J. E., Nieman R. A., Lewis C. E., and Yates A. M. (1989) Stishovite at the Cretaceous-Tertiary boundary, Raton, New Mexico. *Science*, 243, 1182-1184.
- Murdoch J. B., Stebbins J. E., and Carmichael I. S. E. (1985) High-resolution <sup>29</sup>Si NMR study of silicate and aluminosilicate glasses: The effect of network-modifying cations. *Am. Mineral.*, 70, 332-343.
- Oestrike R., Yang W. H., Kirkpatrick R. J., Hervig R. L., Navrotsky A., and Montez B. (1987) High-resolution <sup>23</sup>Na, <sup>27</sup>Al, and <sup>29</sup>Si NMR spectroscopy of framework aluminosilicate glasses. *Geochim. Cosmochim. Acta*, 51, 2199-2209.
- Schneider H., Vasudevan R., and Hornemann U. (1984) Deformation of experimentally shock-loaded quartz powders: X-ray line broadening studies. *Phys. Chem. Minerals*, 10, 142-147.
- Sharpton V. L. and Schuraytz B. C. (1989) On reported occurrences of shock-deformed clasts in the volcanic ejecta from Toba caldera, Sumatra (abstract). In *Lunar and Planetary Science XX*, pp. 992-993. Lunar and Planetary Institute, Houston.
- Smith J. V. and Blackwell C. S. (1983) Nuclear magnetic resonance of silica polymorphs. *Nature*, 303, 223-225.
- Stöffler D. (1971) Coesite and stishovite in shocked crystalline rocks. *J. Geophys. Res.*, 76, 5474-5488.
- Stöffler D. (1984) Glasses formed by hypervelocity impact. *J. Non-Cryst. Solids*, 67, 465-502.
- Vizgirda J., Ahrens T. J., and Tsay F. D. (1980) Shock-induced effects in calcite from Cactus Crater. *Geochim. Cosmochim. Acta*, 44, 1059-1069.
- Yang W. H., Kirkpatrick R. J., Vergo N., McHone J., Emilsson T. I., and Oldfield E. (1986) Detection of high-pressure silica polymorphs in whole-rock samples from a Meteor Crater, Arizona, impact sample using solid-state silicon-29 nuclear magnetic resonance spectroscopy. *Meteoritics*, 21, 117-124.